

Breakpoint Diagnosis of Substation Grounding Grid Using Derivative Method

Aamir Qamar^{1, 2, *}, Nadir Shah¹, Zeeshan Kaleem¹,
Zahoor Uddin¹, and Farooq A. Orakzi¹

Abstract—Grounding grid is responsible for driving lightning and short circuit currents into ground. Faults in substation grounding grid can lead to significant rise in surface potential and ultimately loss to power system and operators. This paper proposes a novel technique based on derivative method to diagnose breakpoints in grounding grid. Derivative of surface magnetic flux density on circle results in peak at conductor's location. Once a conductor is broken the flow of current and surface magnetic field ceases, which is recognized by the absence of peak at corresponding conductor's location. The use of circle even enables this method for diagnosing diagonal branch. Furthermore, the method is analyzed for soil of different resistivities and monolayer and multilayer soils. Simulation results show that the proposed method is feasible for breakpoint diagnosis of grounding grid without excavation.

1. INTRODUCTION

Grounding plays an important role in the safe operation of power system. The element that drives fault currents into earth is known as grounding grid. Grounding grid is a network of horizontal conductors that is made up of metal or metal alloys like copper, steel, galvanized steel, etc.. This grounding grid is buried 0.3 m to 0.5 m (equivalently 12 in to 18 in) deep in the soil [1]. Grounding grid is usually rectangular in shape with mesh spacing 3 m to 7 m. Grounding grid can take any topology depending on substation configuration. Due to the presence of water particles and air gaps in soil, grounding grid is subjected to soil corrosion. With the passage of time grounding grid gets corroded and may break. This limits the efficiency of grounding grid and may get unnoticed due to hidden in soil.

Earlier, excavation was the method to check the status of the grid. However, excavation is costly and time consuming. Recently, fault diagnosis of grounding grid has attracted the attention of many researchers. The methods of grounding grid fault diagnosis developed till date include electrochemical detection method [2], electromagnetic induction method [3–5], transient electromagnetic imaging method [6, 7] and method based on theory of electric circuit [8–10]. Electrochemical detection method determines the degree and rate of corrosion by measuring electrochemical properties between grid conductors and soil. This method works well for corrosion diagnosis but fails to detect breakpoints [2]. [3] used electromagnetic induction method and method of moment (MOM) to develop mathematical formula for calculating leakage current. This method fails to deliver the standard value of leakage current used to differentiate between normal and broken conductor. Dawalibi [4], measured surface magnetic flux density by injecting direct current into down-lead wires. This method is not valid for grounding grid corroded but not broken. Transient electromagnetic imaging (TEM) method calculates resistivity from magnetic field produced by induced eddy currents [6, 7]. This method is applicable for

Received 6 February 2017, Accepted 15 May 2017, Scheduled 31 May 2017

* Corresponding author: Aamir Qamar (aamirqamar@ciitwah.edu.pk).

¹ Department of Electrical Engineering, Comsats Institute of Information Technology, Wah Cantt, Wah 47040, Pakistan. ² State Key Laboratory of Power Transmission Equipment & System Security and New Technology, The Electrical Engineering College, Chongqing University, Chongqing 400044, China.

breakpoint diagnosis but lacks to differentiate between broken conductor and absent conductor. The electric circuit method and surface potential difference method fail because the change in grounding resistance and surface potential is not large enough even if the grid is broken [8–10]. Furthermore, all the above methods were tested for grounding grids with simple rectangular topology.

In this paper, a new method for breakpoint diagnosis of grounding grid is proposed using magnetostatics and derivative method. Derivative method was used previously to locate branch position [11]. Further, derivative method was used to measure the topology of grounding grid [12]. In this study current is injected through vertical conductors in grounding grid which results in surface magnetic flux density. Derivative of surface magnetic flux density on circle is taken to diagnose breakpoints. Presence and absence of peak in magnetic flux gradient graph at conductor's location differentiates between a normal and broken conductor. Moreover, the use of derivative on circle makes the method operational for complex topology containing diagonal conductor. Additionally, the proposed method is examined for parameters like soil resistivity and multilayer soil. The rest of the paper is organized as follows. Section 2 explains the proposed method. In Section 3, simulation and results are discussed. Section 4 concludes the paper with future directions.

2. PROPOSED METHOD ILLUSTRATION

Grounding grid mesh usually contains a lot of branches and nodes. Here a single current carrying conductor is analyzed to explain the method. Fig. 1 shows conductor A of length L placed along y -axis. It is buried at depth h below the surface in a monolayer soil with magnetic permeability μ . DC current I flows through the conductor which according to Biot-Savart's law [13], produces magnetic flux density \vec{B} above the surface. From Fig. 1 the contribution of conductor A to the magnetic flux density \vec{B} at point $P(x, y, h)$ is expressed as:

$$\vec{B} = \frac{\mu}{4\pi} \int_0^L \frac{I dl \hat{a}_y \times \vec{R}}{|R|^3} \quad (1)$$

where \hat{a}_y shows the direction of current I and \vec{R} is the vector directed from differential element dl to point $P(x, y, h)$.

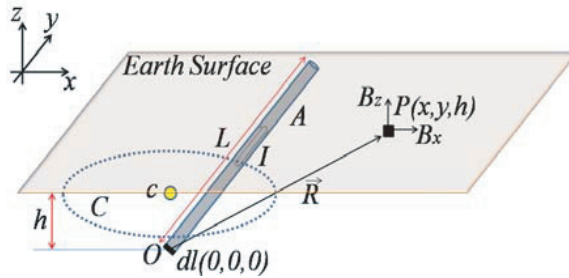


Figure 1. Figure illustrates conductor A buried at depth h below the earth surface in mono-layer soil. DC current I flows through the conductor along y -axis. L is the length of the conductor while magnetic flux density \vec{B} is inspected at point $P(x, y, h)$. C is the circle of derivative with centre point c above the origin O .

Solving Eq. (1) for $\vec{R} = x\hat{a}_x + y\hat{a}_y + h\hat{a}_z$ results in B_x and B_z components of magnetic flux density \vec{B} . Continuing with B_z which is expressed as:

$$B_z = -\frac{\mu I L}{4\pi} \frac{x}{(x^2 + h^2) \sqrt{x^2 + h^2 + L^2}} \quad (2)$$

2.1. Derivative on Circle

Derivative method is used to eliminate ECG artifacts from EEG [14]. Similarly it is used to recompense the frequency and amplitude loss of propagating seismic waves. Furthermore, it is also used to improve

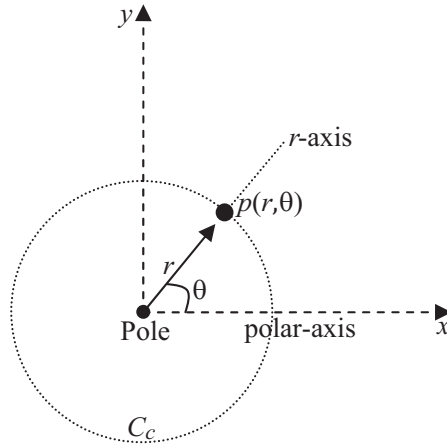


Figure 2. Point $p(r, \theta)$ on circle C_c .

the resolution ratio of GPR data [15, 16].

To understand the role of circle in this method, Fig. 2 is taken into account. As circle is a geometric element in polar coordinates specified by its radius r , angle $\theta = 2\pi$ radians and centre point. Point $p(r, \theta)$ is located on circle C_c only if the circle is centred at the pole of the coordinate system. Mathematically circle is expressed as:

$$C_c = \int_0^{2\pi} r d\theta = 2\pi r \tag{3}$$

To diagnose a broken conductor, location of the conductor is of great significance. For this sake, in Fig. 1 derivative of surface magnetic flux density (B_z) is taken on circle C . This circle C is centred above the origin O so that the condition presented in Fig. 2 is accomplished.

Outcome of derivative on circle C is mathematically expressed as:

$$\frac{dB_z}{d\theta} = \frac{dx}{d\theta} \frac{dB_z}{dx} \tag{4}$$

$$\frac{dB_z}{d\theta} = r \sin \theta \frac{\mu I L}{4\pi} \left[\frac{x^2 (-2x^2 - h^2 - L^2) + h^2 (h^2 + L^2)}{(x^2 + h^2)^2 (x^2 + h^2 + L^2)^{\frac{3}{2}}} \right] \tag{5}$$

Giving a closer look at (5) shows that $\frac{dB_z}{d\theta}$ is maximum at $\theta = \frac{\pi}{2}$ radians and $x = 0$, which represents the location of the buried conductor A. Furthermore, the result of $\frac{dB_z}{d\theta}$ is graphically illustrated in Fig. 3 which is in complete accordance with the mathematical result. Peak of magnetic flux density gradient is located at 1.57 radians which shows the presence of conductor A along y -axis. Due to the fact that magnetic field is equally distributed on either side of a current carrying conductor, its derivate results in a peak at conductor's location. Now this presence of peak at conductor's location reveals the flow of current, a normal conductor. As the conductor is broken, it is unable to conduct. No current means no magnetic field.

3. SIMULATION AND RESULTS

In this section the proposed method is simulated to test its feasibility using COMSOL Multiphysics 4.4. COMSOL works on Finite Element Method (FEM). Under AC/DC module a magnetic and electric field interface is used to perform the simulations.

3.1. Simulation Model

The simulation model features 3×3 square grid made up of steel conductors having conductivity 4.032×10^6 S/m and radius 0.01 m. The dimensions of the grid are $6 \text{ m} \times 6 \text{ m}$ with mesh spacing equals

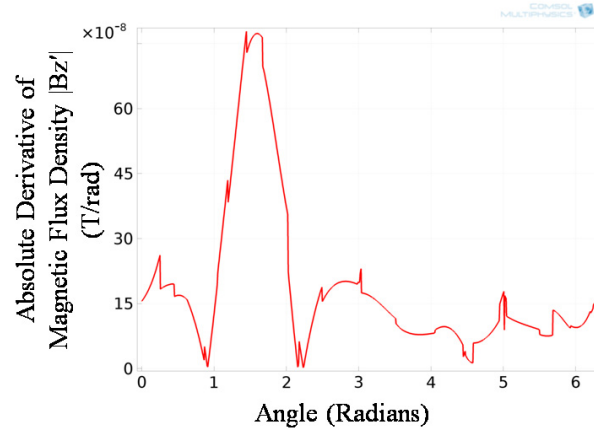


Figure 3. Derivative of magnetic flux density \vec{B}_z on circle C . Location of conductor A is shown by magnetic flux density gradient peak at 1.57 radians. This graph proves the location of conductor A along y -axis.

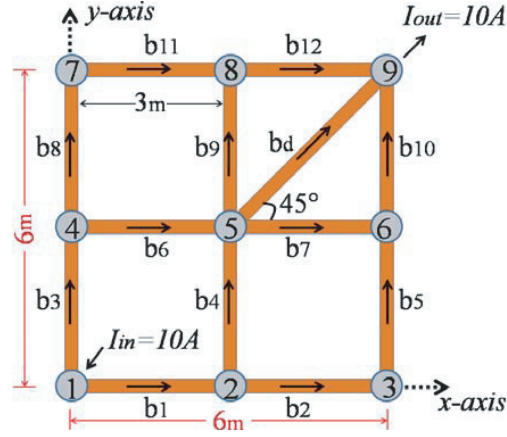


Figure 4. Grounding grid model considered for simulation analysis. Nodes are modelled from 1 to 9 while branches are shown from b_1 to b_{12} . b_d is the diagonal branch making an angle of 45° with branch b_7 . DC current $I = 10$ A is injected from node 1 and received from node 9. Distribution of current is shown by the arrows.

to 3 m. This grid is buried at depth $h = 0.5$ m below earth surface in monolayer soil with resistivity equals to $100 \Omega\text{m}$. Nodes are modelled from 1 to 9 while branches are shown from b_1 to b_{12} . A diagonal branch b_d is connected between node 5 and 9 making an angle of 45° with branch b_7 . DC current $I = 10$ A is injected in node 1 and flown out of node 9. As the current distributes in the grid magnetic flux density $\vec{B}_z(x, y)$ (z -component) is produced above the surface. Fig. 4 illustrates the simulation model.

To do breakpoint analysis of the proposed model two states are considered:

- (i) Normal grounding grid with no breakpoints.
- (ii) Faulty grounding grid with broken cut of 2 cm on branch b_9 .

Derivative of surface magnetic flux density $\vec{B}_z(x, y)$ is taken on circle C_0 centred at node 5. The radius of the circle is taken as 2.43 m. Fig. 5 illustrates circle C_0 and derivative of $\vec{B}_z(x, y)$ on it.

From Fig. 3 it was understood that derivative of surface magnetic flux density decides a normal conductor by presence of magnetic flux density gradient peak at conductor's location and vice versa. Analyzing Fig. 5(b), when the grid is normal (branch b_9 is not broken) derivative of $\vec{B}_z(x, y)$ on C_0

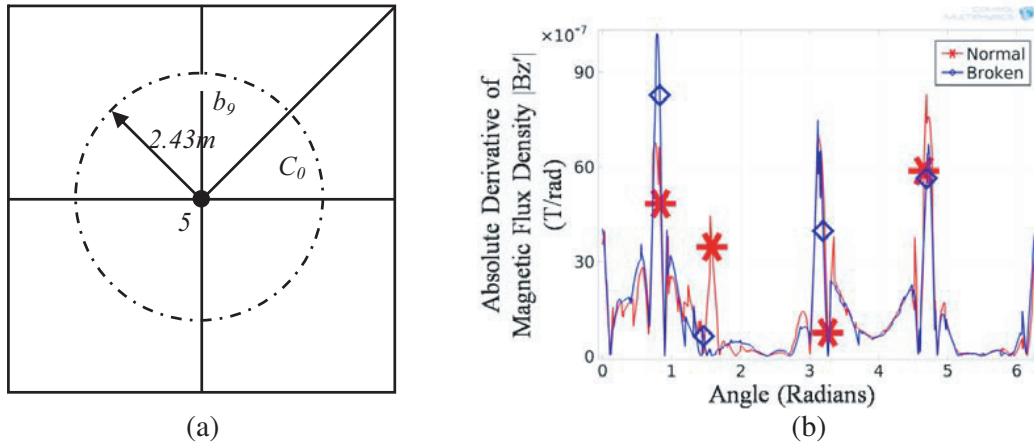


Figure 5. Illustration of derivative method for breakpoint analysis of branch b_9 . (a) Circle C_0 of radius 2.43 m centred at node 5. A broken cut of 2 cm is made on branch b_9 . (b) Graph illustrates outcome of derivative of $\vec{B}_z(x, y)$ on circle C_0 for normal and broken grid. Graph in red shows normal grid when branch b_9 is not broken while graph in blue shows broken grid when branch b_9 is broken.

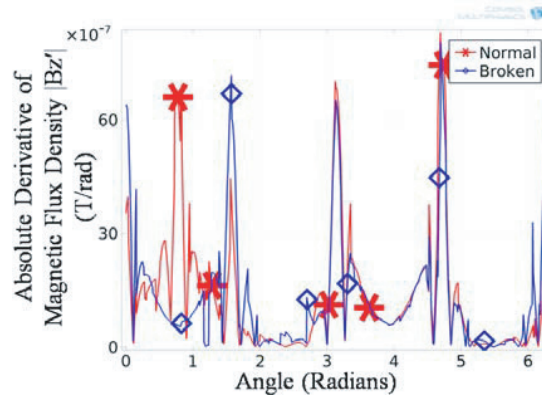


Figure 6. Breakpoint analysis of diagonal branch b_d . Normal graph in red shows peak at 0.78 radians. Broken graph in blue has only four peaks. Peak at 0.78 radians is missing which indicates that no current flows in branch b_d and is broken.

gives five peaks at 0 radians (branch b_7), 0.78 radians (branch b_d), 1.57 radians (branch b_9), 3.14 radians (branch b_6), and 4.71 radians (branch b_4). The presence of these peaks assures that the corresponding branches are not broken. On the contrary, peak at 1.57 radians (branch b_9) is missing. This shows that branch b_9 is broken. The same procedure is repeated for diagonal branch b_d . In case of normal condition (branch b_d not broken) peak is present at 0.78 radians which is the location of branch b_d on C_0 . When a broken cut of 2 cm is introduced to branch b_d , its status is identified by the absence of peak at its location. Breakpoint analysis of branch b_d is shown in Fig. 6.

As grounding grid is buried in soil, influence of varying soil resistivity on the proposed method is tested. Furthermore, the soil can be monolayer or multilayer. The method is also simulated for multilayer soil.

3.2. Effect of Soil Resistivity

Resistivity of soil ranges from few ohm-meters to hundred ohm-meters depending on the location and weather conditions. The derivative method of breakpoint diagnosis is simulated for varying soil resistivity. The soil resistivity values taken in the simulation are $20\ \Omega\text{m}$, $100\ \Omega\text{m}$ and $1000\ \Omega\text{m}$. Moreover,

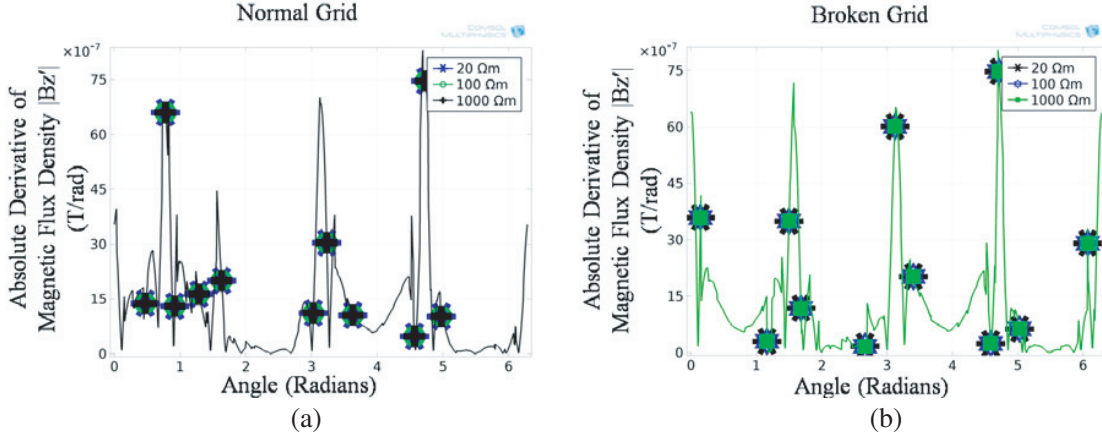


Figure 7. Effect of soil resistivity on derivative method. (a) Influence of soil resistivity on derivative method. The graph is the outcome of $|\vec{B}'_z|$ on circle C_0 for normal grid. The values of soil resistivities considered are $20 \Omega\text{m}$, $100 \Omega\text{m}$ and $1000 \Omega\text{m}$. (b) Influence of soil resistivity on derivative method. The graph is the outcome of $|\vec{B}'_z|$ on circle C_0 for broken grid (diagonal branch b_d). The values of soil resistivities considered are $20 \Omega\text{m}$, $100 \Omega\text{m}$ and $1000 \Omega\text{m}$.

the simulation is performed for normal and broken grid.

Analyzing Fig. 7, soil resistivity has no impact on the derivative method. The location of $|\vec{B}'_z|$ peak and even its amplitude remains unchanged for either value of soil resistivity. This may be due to the fact that the conductivity of soil is too low as compare to the conductivity of steel conductors ($4.032 \times 10^6 \text{ S/m}$). The largest percentage difference for Fig. 7(b) is $3.35 \times 10^{-14}\%$.

3.3. Multilayer Soil

Resistivity of soil varies with depth from the surface. The proposed method is simulated for two-layer soil. Fig. 8 illustrates two-layer soil model. Depth of upper layer is taken as 0.2 m while depth of lower layer is taken as 0.4 m . The values of resistivity considered are $100 \Omega\text{m}$ and $1000 \Omega\text{m}$. Fig. 9 shows the effect of multilayer soil on the proposed method. Simulations are performed for broken grid (diagonal branch b_d) considering positive and negative reflection factor K . Reflection factor K is mathematically expressed as [17]:

$$K = \frac{\rho_2 - \rho_1}{\rho_1 + \rho_2} \quad (6)$$

where ρ_1 is the resistivity of upper soil layer and ρ_2 is the resistivity of lower soil layer.

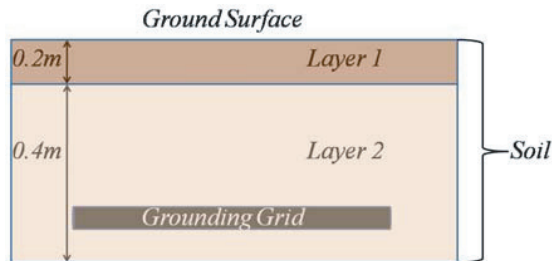


Figure 8. Diagram showing grounding grid buried in two-layer soil. The thickness of layer 1 (upper layer) is 0.2 m and depth of layer 2 (lower layer) from layer 1 is 0.4 m . Resistivity of the layers is taken as $100 \Omega\text{m}$ and $1000 \Omega\text{m}$ considering positive and negative reflection factor.

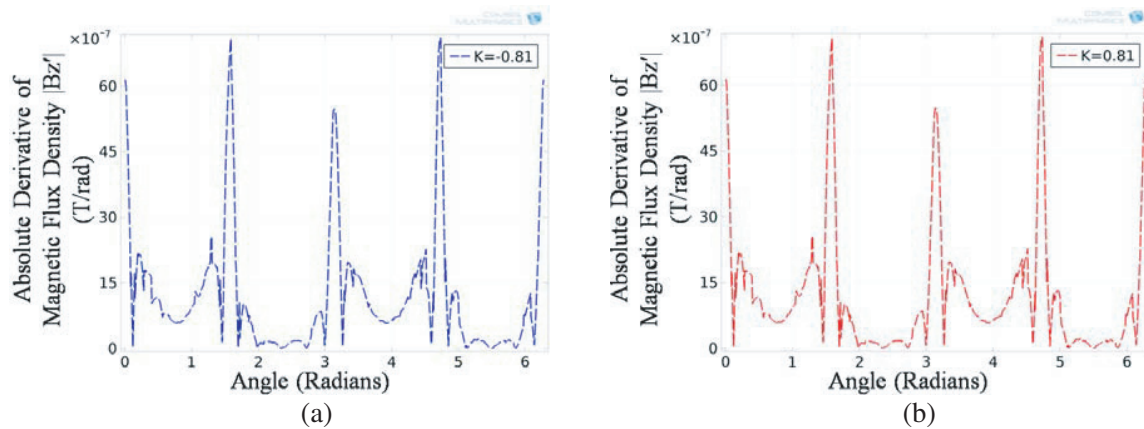


Figure 9. Analysis of derivative method using multilayer soil. (a) Result of $|B'_z|$ on circle C_0 when the grid is buried in two-layer soil. Reflection factor $K = -0.81$ ($\rho_1 = 1000 \Omega\text{m}$ and $\rho_2 = 100 \Omega\text{m}$). (b) Result of $|B'_z|$ on circle C_0 when the grid is buried in two-layer soil. Reflection factor $K = 0.81$ ($\rho_1 = 100 \Omega\text{m}$ and $\rho_2 = 1000 \Omega\text{m}$).

A closer observation of Fig. 9 shows that derivative method of breakpoint diagnosis equally works for grounding grid buried in multilayer soil. The results are consistent regarding the amplitude and location of peaks. Moreover, the method is also independent of reflection factor K .

4. CONCLUSION

In this paper, a novel technique based on derivative method for breakpoint diagnosis of substation grounding grid is presented. Using the derivative of surface magnetic flux density on circle, this method not only is applicable to simple branches but also diagnoses broken diagonal branch. This is a clear advantage of the proposed method over other existing methods for breakpoint diagnosis. The proposed method is investigated for parameters such as varying soil resistivity and multilayer soil. From the results it is determined that the method is not affected by varying soil resistivity and is applicable for multilayer soil. Results show that the method is feasible for diagnosing breaks in grounding grid without excavation. Secondly, the method is feasible for grid topology having diagonal branch.

Strong electromagnetic interference (EMI) in substation can affect the performance of our proposed approach. Therefore, we would like to address this issue in our future work.

REFERENCES

1. "IEEE Guide for Safety in AC Substation Grounding," *IEEE Standard 80-2000*.
2. Zhang, X., X. Zhao, Y. Wang, and N. Mo, "Development of an electrochemical in situ detection sensor for grounding grid corrosion," *Corrosion*, Vol. 66, No. 7, 076001-1–076001-7, Jul. 2010.
3. Zhang, B., Z. Zhao, X. Cui, and L. Li, "Diagnosis of breaks in substation's grounding grid by using the electromagnetic method," *IEEE Trans. Magn.*, Vol. 38, 473–476, Mar. 2002.
4. Dawalibi, F., "Electromagnetic fields generated by overhead and buried short conductors, Part 2 — Ground networks," *IEEE Transactions on Power Delivery*, Vol. 1, 112–119, Oct. 1986.
5. Liu, Y., X. Cui, and Z. Zhao, "A magnetic detecting and evaluation method of substation's grounding grids with break and corrosion," *Front. Electr. Electron. Eng. China*, Vol. 5, 501–504, Dec. 2010.
6. Yu, C, Z. Fu, X. Hou, H.-M. Tai, and X. Su, "Break point diagnosis of grounding grids using transient electromagnetic apparent resistivity imaging," *IEEE Transactions on Power Delivery*, Vol. 30, 2485–2491, Feb. 2015.

7. Yu, C, Z. Fu, Q. Wang, H.-M. Tai, and S. Qin, "A novel method for fault diagnosis of grounding grids," *IEEE Transactions on Industry Applications*, Vol. 51, 5182–5188, Jun. 2015.
8. Zeng, R., J. He, J. Hu, G. Lu, and B. Luo, "The theory and implementation of corrosion diagnosis for grounding system," *37th IEEE IAS Annual Meeting*, Vol. 2, 1120–1126, Oct. 2002.
9. Zhu, X., L. Cao, J. Yao, L. Yang, and D. Zhao, "Research on ground grid diagnosis with topological decomposition and node voltage method," *2012 IEEE Congress Engineering and Technology (S-CET)*, 1–4, Xi'an, China, May 2012.
10. Yuan, J., H. Yang, L. Zhang, X. Cui, and X. Ma, "Simulation of substation grounding grids with unequal-potential," *IEEE Trans. Magn.*, Vol. 36, 1468–1471, Jul. 2000.
11. Wang, X., C. Li, W. He, F. Yang, D. Yao, and X. Kou, "Topological measurement and characterization of substation grounding grid based on derivative method," *International Journal of Electrical Power and Energy Systems*, 2014.
12. Qamar, A., F. Yang, W. He, A. Jadoon, M. Z. Khan, and N. Xu, "Topology measurement of substation's grounding grid by using electromagnetic and derivative method," *Progress In Electromagnetics Research B*, Vol. 67, 71–90, May 2016.
13. Ida, N., *Engineering Electromagnetic*, 3rd Edition, Springer, 2015.
14. Lee, K. J., C. Park, and B. Lee, "Elimination of ECG artifacts from a single-channel EEG using sparse derivative method," *IEEE International Conference on Systems, Man, and Cybernetics*, 2384–2389, 2015.
15. Yu, H. and X. Ying, "Derivative seismic processing method for GPR data," *IEEE Int. Geosci. Rem. Sens.*, 145–7, 1997.
16. Liu, Q., "Sensitivity and Hessian matrix analysis of power spectral density functions for uniformly modulated evolutionary random seismic responses," *Finite Elements in Analysis and Design*, Vol. 48, 1370–1375, 2012.
17. "IEEE Guide for Safety in AC Substation Grounding", *IEEE Standard 80-2013*.